
Sevilla

# DYNAMIC ANALYSIS OF NON-SINUSOIDALLY SUPPLIED INDUCTION MACHINE BASED ON THE FINITE ELEMENT METHOD.

R. De Weerdt, K. Hameyer, R. Belmans

Katholieke Universiteit Leuven
Dept. EE, Div. ESAT/ELEN

**Abstract: The analysis of a squirrel-cage induction motor based on the finite element calculations is described. The finite element calculations are used to generate an extended motor model describing the motor as a set of coupled windings. The significant difference with conventional motor models as the d-q-model is that the inductance matrix in the model includes saturation and motor slotting in a natural way. Both are described as a ripple on the inductances. Once the model is calculated, it is used in simulations by solving the set of voltage differential equations describing the coupled windings. Simulations are performed, both with and without motion. Voltage supply can be both sinusoidal and time dependent when an invertor is used.**

Keywords: squirrel-cage induction motor, finite element analysis, simulation, inverter supply, motion

## INTRODUCTION

The induction motor analysis is mainly based on the d-q-model or the equivalent circuit. Parasitic effects such as audible noise and vibrations cannot be desribed using these models since the parameters in both models are considered to be constant. Therefore, simulations with those models will only produce frequency components caused by the voltage supply or the motion equation. The real motor behaves different: several harmonics are introduced in the spectrum of current and torque even at sinusoidally supplied voltage. An additional disadvantage of the classical approach is that empirical formulae are used during the design process and thus also during the motor analysis [1]. Deriving these empirical formules implies the constructing of prototypes, a both costly and time-consuming task. The analytical or empirical approach is also limited in providing a motor model that is accurate enough to meet the requirements of advanced control algorithms such as vector control without speed or position feedback. Using analytical or empirical formulae it is impossible to split the leakage reactance into a rotor- and a stator part.

A model based on finite element calculations can provide a more detailed description having the following advantages for the industry.

A finite element solution provides a more unbiased solution since no measurements on prototypes are required. An optimisation towards use of material and power density can thus be performed faster and less expensive.

The model presented here incorporates parasitic effects such as saturation and motor slotting. The effects of saturation and slotting on the current- or torque spectrum can be examined in a quantitative way. In the classical analysis, this is done using a Fourier-analysis of the airgap field [2]. This approach only results in a qualitative analysis since several approximations have to be made to derive the analytical expression of the airgap field.

## DESCRIPTION OF THE MODEL

For deriving the motor model, the motor is considered to be a set of coupled windings. Each winding can be represented by a differential equation:

$$[u] = [R][i] + \frac{d}{dt}[\psi] \qquad (1)$$

$$[\psi] = [L][i]$$

where [R] is the resistance matrix, [i] the current vector, [u] the applied voltage vector, [ψ] the vector describing the flux linkage and [L] the inductance matrix. The motors modelled are four-pole motors having 48 stator slots and 40 rotor slots. Due to symmetry in the model, only one pole pitch is considered. The applied voltage [u] is modified properly taking the number of parallel branches into

account and the stator circuit being Y or Δ-connected. Each of the ten rotor bars per pole pitch is considered as a separate rotor phase. Therefore, the model consists of 13 phases.

The 13x13 inductance matrix [L] in (1) is calculated using a two dimensional finite element model. Saturation is taken into account employing a previously developped iterative process [3]. The process uses both, the static (non-linear) and the time-harmonic (linear) solution to evaluate saturation in the motor for a given excitation on one hand and the induced currents (including skin effect) on the other. This procedure is found to give simular results to other methods described in the literature. There only time-harmonic solutions are used [4]. As a result of the iterative process, the reluctivity in each element of the model for a given rotorposition and excitation is obtained.
Using the extracted reluctivities, the inductance matrix [L] is calculated as described in [3]. For each of the 13 phases, a linear problem is defined with a current of 1 A per phase. The problem is solved using the extracted reluctivities as a working point and the flux through the 13 phases is determined. Since a 1 A current is used, these flux linkages immediately are representing the mutual inductances. The inductances are calculated as described in [5].
Clearly, using the above described method for computing the inductances, an inductance is defined as the instantaneous ratio of the flux linkage through a certain phase and the current causing this flux. From the set of equations (1) it is obvious that this is the correct definition to apply.
When the above described procedure is repeated for different rotor positions and excitations, the variation of the inductances can be examined. When the rotor position is varied, the excitation has to be varied accordingly. When the rotor is rotated more than $\alpha_m$ degrees, the excitation shifts to $\alpha_e$ degrees:

$$\alpha_e = \frac{p\alpha_m}{(1-s)} \qquad (2)$$

(p: number of pole-pairs, s: slip)

## RESULTS AND INTERPRETATION

The inductance matrices are calculated for different motors and different load situations. For no-load and rated load, it is found that only one third of a period of the excitation has to be modelled. This provides sufficient data to construct the variation of the inductances during the remaining period. For locked rotor calculations, half a period has to be modelled. Figures 1 to 3 show some of the simulation results in the time-domain.

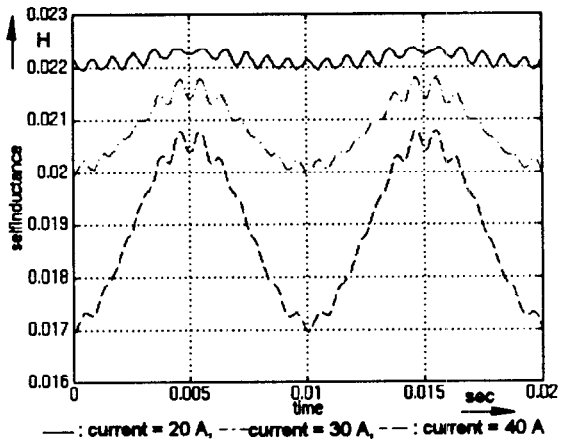


Figure 1: Variation of the self inductance of a stator phase during one period for different values at no-load.

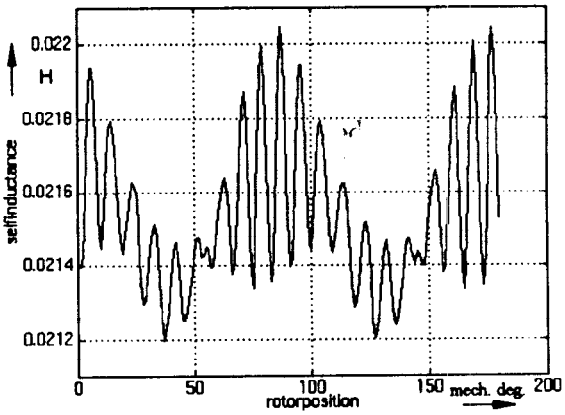


Figure 2: Variation of the self inductance of a stator phase during one period at rated condition.

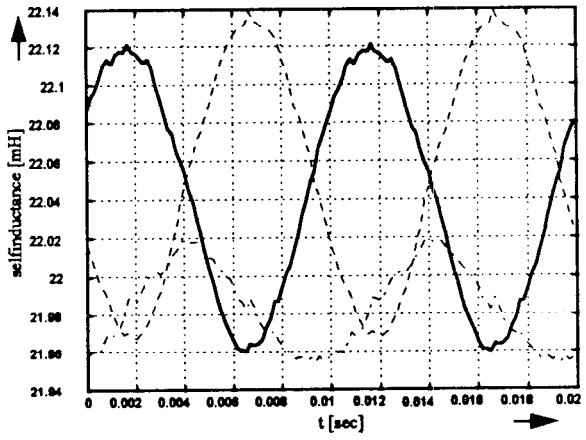


Figure 3: Variation of the self inductance of the three stator phases during one period at locked rotor situation.

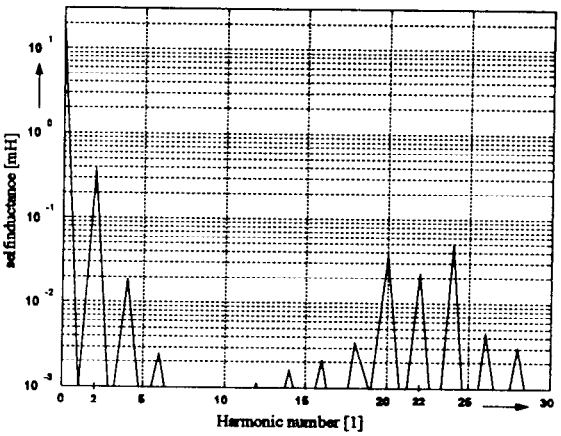


Figure 4: Harmonic content of the stator self inductance at rated condition

Figure 4 shows the harmonic content of the self inductance from figure 2. In all load situations (figures 1 to 3) a second harmonic ripple can be detected in the inductances. This ripple is caused by saturation of the motor iron. From the no-load situation (figure 1) it can be seen that, if saturation increases (e.g. higher value of the no-load current), the amplitude of the second harmonic increases and the average inductance decreases. From physical considerations it is known that the ripply caused by saturation can be described as a second harmonic of the supply frequency and therefore, as a function of time t. The other higher harmonics present in the inductances of figures 1 to 3, are caused by rotor- and stator slotting and can be described as a function of the rotorposition θ.
All inductances in the matrix [L] of equation (1) can be described in a simular way. For instance it is noted that the rotor inductances (both self inductances of the rotor phases and mutual inductances) are described by a constant value in combination with a 24th harmonic component. Clearly, this harmonic component is caused by stator slotting since the stator has 24 slots per pole pair. The stator self- and mutual inductances contain a 20th, 22th and 24th harmonic component due to rotor slotting and the distributed stator winding (see figure 4). Therefore, the self inductance of a stator phase $L_s$ will be described as

$$L_s = L_0 + L_2\cos(2\omega_n + \alpha_2) + L_{20}\cos(20p\theta + \alpha_{20}) + L_{22}\cos(22p\theta + \alpha_{22}) + L_{24}\cos(24p\theta + \alpha_{24}) \quad (3)$$

($\omega_n$: the supply pulsation, $L_n$ and $\alpha_n$: magnitude and phase angle of the $n^{th}$ harmonic component) $L_n$ and $\alpha_n$ are obtained by performing a discrete Fourier transformation on the inductances. Using this approach, the inductances calculated for a distinct number of rotorpositions are transferred into a continuous function that can be evaluated at any desired instance.

This representation of inductances is significantly different from traditional models as there are the α–β-model (two-phase model in a reference frame fixed to the stator) or the d-q-model (two-phase model in a reference frame rotating at synchroneous speed). In those models, all parameters are considered to be independent of time, and only some elements are a function of the rotorposition θ. Simulations with those models cannot produce harmonics in the current or torque due to saturation or slotting.
Since the inductances are represented as continuous functions of t and θ as in (3), the influence of each harmonic component can be examined by including or excluding it in the calculations. If all harmonics are omitted, the model becomes an extended version of the more classical two-phase models. A transformation to such a two-phase model then becomes trivial using a Park transformation on both, rotor and stator equations. The transformation from an n-phase system to a two phase system with preservation of the power can be described by:

$$[A] = \sqrt{\frac{2}{n}}\begin{bmatrix} \cos\left(0\frac{n}{2\pi}\right) & \sin\left(0\frac{n}{2\pi}\right) \\ \cos\left(1\frac{n}{2\pi}\right) & \sin\left(1\frac{n}{2\pi}\right) \\ \cdots & \cdots \\ \cos\left((n-1)\frac{n}{2\pi}\right) & \sin\left((n-1)\frac{n}{2\pi}\right) \end{bmatrix} \quad (4)$$

For the transformation, it is assumed that the first phase of the two phase system is aligned with the first phase of the n-phase system. Furthermore, no homopolar currents may exist.

## SIMULATIONS

When the inductances are calculated as described above and are transformed into continuous functions, the set of equations (1) can be solved. To do so, (1) is transformed into one equation of the form $\frac{dx}{dt} = f(x,t)$. Two possibilities exist for this transformation.

Either the current vector [i] or the flux vector [ψ] is taken as the unknown

$$\frac{d[i]}{dt} = [L]^{-1}\left([u] - [R][i] - \frac{d[L]}{dt}[i]\right) \quad (5)$$

$$\frac{d[\psi]}{dt} = [u] - [R][L]^{-1}[\psi] \quad (6)$$

Considering the fluxes as unknowns (6) results in a numerically better conditioned set of equations. The

main reason why (5) is more difficult to solve accurately, compared to (6), is the appearance of the derivative of the inductance matrix in (5). However, it is not impossible to consider (5) to be solved as shown in [6]. There it was assumed that the speed is constant. Here, (6) will be used to describe the motor during speed variations also. The computation of the instantaneous currents can be performed without difficulties during the simulation or afterwards since the inductance matrix [L] is evaluated at each time-step of the simulation. Two types of simulations are performed.

Constant Speed

When the speed is considered to be constant, the rotor position $\theta$ in (3) can be replaced by $\omega_m t$, $\omega_m$ being the mechanical speed. This approach is used for locked rotor simulations ($\omega_m = 0$) or to compute the steady-state torque-slip characteristic. The speed is fixed during the simulations, the unstable region of the characteristic can be computed also. The set of equations (6) is solved using the trapezium-rule with NEWTON-iterations. The advantage of this method is that the region of stability of the method corresponds to the region of stability of the solved system. A disadvantage is that the JACOBIAN of the system has to be calculated. The JACOBIAN of the system described by (6) is $[1]-[R][L]^{-1}$, which is a fully occupied matrix. Several modifications do exist for the NEWTON-RAPHSON algoritm. Often, the JACOBIAN is calculated outside the iteration loop, only once. This is also done here. Futhermore, the calculations show, that the JACOBIAN can be simplified by taking only the diagonal elements of $[1]-[R][L]^{-1}$. The torque T developped by the motor can be evaluated at each time-step using [7].

$$T = \frac{1}{2}[i]^T \frac{\partial L}{\partial \theta}[i] \qquad (7)$$

Variable Speed

To allow the speed to be variable means adding the motion equation to the set of equations to be solved. The motion equation is mainly described as a second order differential equation. This equation is split into two first order equations.

$$\frac{d\theta}{dt} = \omega$$
$$\frac{d\omega}{dt} = \frac{T - T_{load} - B\omega}{J} \qquad (8)$$

($\theta$: rotor position, T: generated torque , $T_{load}$: load torque, J: moment of inertia B: friction coefficient). The system is now described by equations (6), (7) and (8). The computation of the JACOBIAN becomes rather complicated due to the presence of the generated torque (7). Therefore, the simulations at variable speed are performed using a fourth order RUNGE-KUTTA method. Caution must be taken using this method since it can produce an unstable solution for a stable system if the solution tolerance is set too high.

For both types of simulations, the input voltage vector [u] may be a set of sinusoidal voltages or the time depending value of an inverter voltage. The end effects of the induction motor (end winding- and end ring impedance) are included in the resistance matrix [R] and the inductance matrix [L] by an increased value of resistance or leakage inductance. The applied end effect parameters are calculated using both two and three dimensional finite element models [8] in order to avoid the use of empirical formulae.

RESULTS

The methods described above are used to perform serveral simulations. For the first simulation, the speed is constant. As menioned, fixing the speed to a constant value allows the calculation of the torque-speed characteristic, even in the unstable region. The following figures show the calculated characteristic with the harmonics due to slotting and saturation removed. The x-marks represent measured values of the mechanical torque.

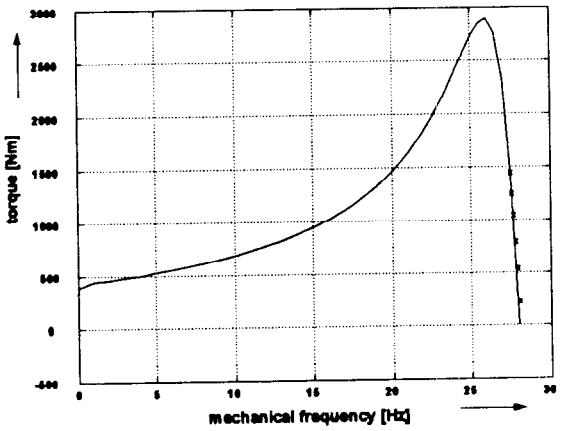


Figure 5: Calculated torque-speed characteristic compared with measured values.

As can be seen in the close-up of the descending slope of the characteristic (figure 6) that the measured values (for a given frequency) are in good agreement with the calculated values. It is obvious that the calculated values are higher since they represent the torque generated by the motor while the measurement data represent the torque measured at the shaft. Due to friction, the generated torque is larger than the mechanical torque.

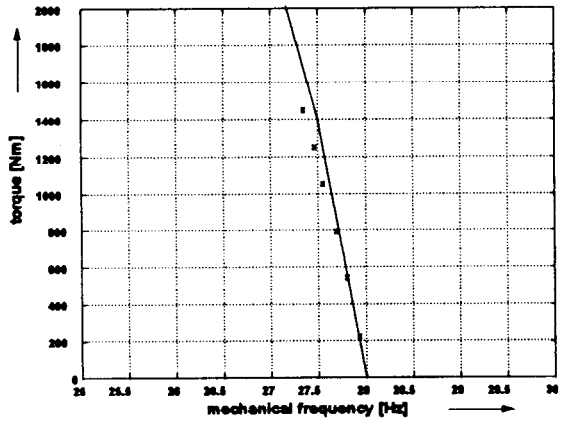


Figure 6: Close-up of the torque-speed characteristic, calculated and measured values of torque

In figures 7 and 8, the influence of the applied voltage is demonstrated. The figures show the frequency spectrum of the no-load current when supplied by a sinusoidal (fig. 7) and a square-wave voltage (fig. 8).

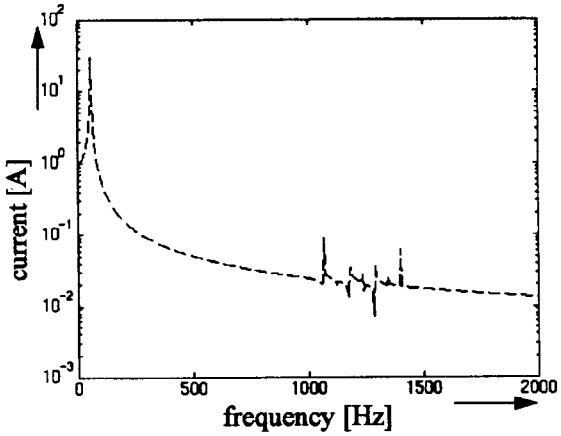


Figure 7: Frequency spectrum of the no-load current with sinusoidal supply voltage.

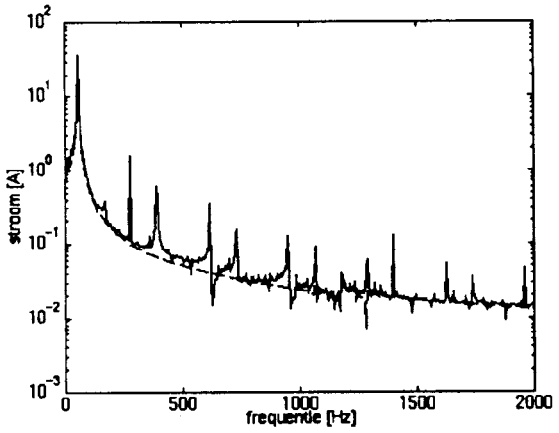


Figure 8: Frequency spectrum of the no-load current with square-wave supply voltage, the dotted line is the spectrum with sinusoidal supply.

The figures show a significant difference in the harmonic content of both currents. If a non-sinusoidal voltage is applied, the harmonics caused by the inverter are found to be more important than the harmonics due to slotting. A comparison with measurements shows good agreement. Both, for load and no-load, the measured frequency components are appearing in the simulations [3]. Comparing the magnitudes of measured and calculated harmonics, it is found that the calculations overestimate the harmonic content of the currents. One of the reasons is that during simulations, the supply voltage is considered not to have an internal impedance. In reality however, it is found that the same harmonics as existing in the current, are also found in the supply voltage. The influence of this internal impedance is a reduction of the harmonic content of the current (figure 9).

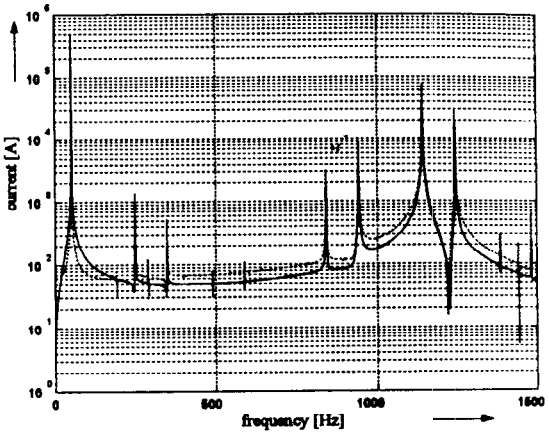


Figure 9: Stator current spectrum at rated speed with sinusoidal supply voltage both with (———) and without (- - - - -) internal impedance.

The simulation with the internal impedance is performed very elementary. The supply voltage is modelled as a zero-impedance voltage source E in series with an inductance L. The inductance L and voltage E are chosen in order to obtain the rated supply voltage U at the voltage source terminals at rated current (figure 10). An inductance value of 2 mH is chosen for L.

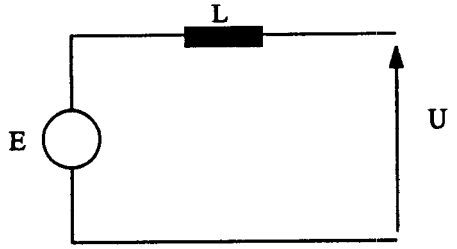


Figure 10: Modelling of voltage source with non-zero internal impedance.

Modelling the supply voltage with an internal impedance reduces the harmonic content of the current

significantly. The harmonic components with the internal impedance are more than twice as low (figure 9).

Figure 11 shows the influence of motion on the calculations. Considering the motion equation has an effect on both, torque- and current spectrum. The difference with constant speed simulations is depending on the parameters in the motion equation. Clearly, an increased inertia J results in a solution that agrees better with a constant speed assumption.

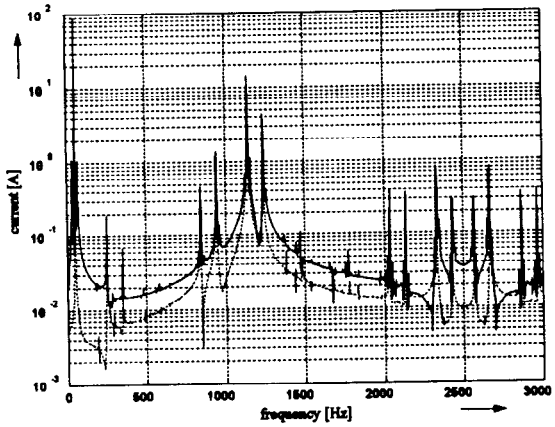


Figure 11: Frequency spectrum of stator current at constant speed (- - - - - -) and with inclusion of motion (———)

Simulations show an increase in harmonic components in the current spectrum if motion is included. However, the increase is less obvious as the variation obtained when the internal impedance of the voltage source is taken into account.

## CONCLUSIONS

An extended motor model based on finite element calculations is presented. The model includes the effect of saturation in a natural way by a ripple on the inductances of the inductance matrix [L]. Simulations with and without motion are performed. The influence of this inclusion in comparison with constant speed assumption is examined. The influence of modelling the supply voltage without internal impedance on the harmonics is shown. Good qualitative agreement in the harmonics is found when compared to measurements. The transformation to the classical motor models is possible and explained.


## ACKNOWLEDGEMENTS

The authors express their gratitude to the Belgian Ministry of Scientific Research for granting the IUAP No. 51 on Magnetic Fields, To Holec, Machines & Apparaten, Ridderkerk and to the Council of the Belgian National Science Foundation.


## REFERENCES


[1] Nürnberg W., "*Die Asynchronmaschine,*" Springer Verlag Berlin Heidelberg New York, 1952.

[2] Liwschitz-Garik, "*Alternating Current Machines,*" D. Van Nostrand Company Ltd., 1946.

[3] Belmans R., De Weerdt R. and Tuinman E., "Combined field analysis techniques and macroscopic parameter simulation for describing the behaviour of medium-sized squirrel-cage induction motors fed with an arbitrary voltage," EPE Brighton, September 1993, pp. 413-418.

[4] Vassent E., Meunier G. and Sabonnadiere J.C.: "Simulation of induction machine operation using complex magnetodynamic finite elements," *IEEE Trans. on Magnetics*, Vol. 25, No. 4, 1989, pp. 3064-3066.

[5] Lowther D.A. and Silvester P.P.: "*Computer-Aided Design in Magnetics,*" Springer-Verlag, New York, 1985.

[6] Mukherjee S., Adams G.E.: "FEM analysis of inverter-induction motor rotor conduction losses," *IEE Trans. on Energy Conversion*, Vol. 4 No. 4, 1989, pp. 671-677.

[7] Krause P.C., "*Analysis of Electric Machinery,*" McGraw-Hill Book Company, 1986.

[8] Freeman E.M., "*MagNet User Guide,*" Infolytica Montreal, 1994.